MEMS GYROSCOPE PERFORMANCE COMPARISON USING ALLAN VARIANCE METHOD

Martin Vagner
Doctoral Degree Programme (1), FEEC BUT
E-mail: xvagne04@stud.feec.vutbr.cz

Supervised by: Petr Benes
E-mail: benesp@feec.vutbr.cz

Abstract: MEMS accelerometers and gyroscopes are suitable for the inertial navigation of mobile robots due to the low price, small dimensions and light weight. The main disadvantage in a comparison with classic sensors is a worse long term stability. For a simple long term stability analysis the Allan variance method could be used. The topic of this article is a measurement of the Allan variance for MEMS gyroscopes. Results based on the measurement of three different gyroscopes are presented.

Keywords: MEMS, gyroscope, Allan variance, stability, bias, random walk

1 INTRODUCTION

The rate gyroscope output is disturbed by two main groups of errors. The first group represents deterministic errors like a constant bias or a nonlinearity. These errors can be corrected by the calibration based on a laboratory measurement. The second group of errors contains unpredictable stochastic processes like angle random walk, bias instability, rate random walk or drift ramp. They appear on the output as a noise or a slow change of parameters in time. The contribution of these errors at a specific time can not be precisely predicted, which causes the degradation of a gyroscope performance.

For the analysis of stochastic processes in a conjunction with gyroscopes, two methods are mainly used. They are defined by IEEE std 952-1997 [1]. The first and more complex one is the power spectral density (PSD). The latter method is the Allan variance (AV).

PSD is the transformation of time data series to the frequency domain. Power spectral densities are statistical measures, which can be estimated from real data by averaging over the results from many measurements. The result can be interpreted as the relative probability of a signal at a given frequency at any point in time.

AV is the method of analysis of stochastic processes in a time domain. It was originally designed for the statistics of atomic frequency standards [2]. The main advantage of AV in a comparison with PSD is a lower computational complexity. On the other hand, there is a problem in interpretation of some kinds of noises, which appear in the same way. However, a solution is using the modified Allan variance. Because of the problem analogy, the AV method could be used for the investigation of gyroscopes as well. First it was used for laser ring gyro [4].

2 ALLAN VARIANCE

As mentioned, AV is a method of analysis in a time domain. It describes variance of a signal as a function of averaging time. Frequently, the Allan variance term is also used to refer to its square root. We can also often see the term cluster analysis, which expresses the principle of operation. In the IEEE 952-1997 [1] standard, the Allan variance $\sigma^2_\Omega(\tau)$ is described for an angle velocity Ω as

follows:

$$\theta(t) = \int^{t} \Omega(t')dt' \tag{1}$$

$$\overline{\Omega}_k(\tau) = \frac{\theta(t_k + \tau) - \theta(t_k)}{\tau} \tag{2}$$

$$\sigma^2_\Omega(\tau) = \frac{1}{2}\left\langle \left(\overline{\Omega}_{k+1} - \overline{\Omega}_k\right)^2 \right\rangle, \tag{3}$$

where τ is an averaging time and operator $\langle ... \rangle$ is defined as an infinite time average [2]:

$$\langle f(t) \rangle = \lim_{T\to\infty} \frac{1}{T} \int_{-T/2}^{T/2} f(t)dt \tag{4}$$

For a finite number of samples N, the Allan variance σ^2_Ω can be estimated as [3]:

$$\sigma^2_\Omega(M) \cong \frac{1}{2(K-1)} \sum_{k=1}^{K-1} \left(\overline{\omega}_{k+1}(M) - \overline{\omega}_k(M)\right)^2, \tag{5}$$

where M means number of samples in one cluster, $K = N/M$ number of clusters, and $\overline{\omega}_k(M)$ is average in cluster k. For this equation, the recursive formula can be derived, as described in [3]. The relation between power spectral density and Allan variance is expressed as [1]:

$$\sigma^2_\Omega(\tau) = 4\int_0^\infty S_\Omega(f) \frac{\sin^4(\pi f\tau)}{(\pi f\tau)^2} df \tag{6}$$

There is no inversion formula.

2.1 ASYMPTOTIC PROPERTIES

The output of gyroscope is affected by several types of noise. The four basic noise terms are angle random walk, bias instability, rate random walk, and rate ramp. If the noise sources are statistically independent, then the computed Allan variance is a sum of the squares of each error type:

$$\sigma^2(\tau) = \sigma^2_{arw}(\tau) + \sigma^2_b(\tau) + \sigma^2_{rrw}(\tau) + \sigma^2_{rr}(\tau) \tag{7}$$

Because of different asymptotic properties they appear in the log-log plot of $\sigma^2(\tau)$ with the different slopes.

2.1.1 ANGLE RANDOM WALK (ARW)

ARW is high frequency noise and it can be observed as the short-term variation in the output. After performing an integration, it causes random error in angle with distribution, which is proportional to the square root of the elapsed time. As described at [1] ARW appears in PSD as:

$$S_\Omega(f) = N^2 \tag{8}$$

Substituting (8) into the equation (6) we get:

$$\sigma^2_{arw}(\tau) = \frac{N^2}{\tau} \tag{9}$$

The equation (9) shows that the slope of $\sigma(\tau)$ log-log plot is -0.5 and the coefficient N can be obtained from the plot at $\tau = 1$ (fig. 1).

2.1.2 BIAS INSTABILITY

The bias instability has an impact on the long-term stability. It is slow fluctuation of output so it appears in low frequencies as $1/f$ noise. Bias instability determines the best stability that could be achieved with fully modeled sensor and active bias estimation. PSD associated with this noise is [3]:

$$S(f) = \begin{cases} \frac{B^2}{2\pi f} & \text{if } f \leq f_0 \\ 0 & \text{if } f > f_0 \end{cases} \tag{10}$$

B is the bias instability coefficient and f_0 is the cutoff frequency. By substituting (10) into (6) and performing the integration we get:

$$\begin{aligned} \sigma_b^2(\tau) &= \frac{2B^2}{\pi}\left[\ln 2 - \frac{\sin^3 \pi f_0 \tau}{2(\pi f_0 \tau)^2}(\sin \pi f_0 \tau + 4\pi f_0 \tau \cos \pi f_0 \tau) + C_i(2\pi f_0 \tau) - C_i(4\pi f_0 \tau)\right] \\ &= \left(\frac{B}{0.6648}\right)^2 \text{ for } \tau >> \frac{1}{f_0}, \end{aligned} \tag{11}$$

where meaning of $C_i()$ is cosine-integral function. In the figure 2, the square root of Allan variance for bias instability is depicted. The coefficient B can be determined from the region with zero slope.

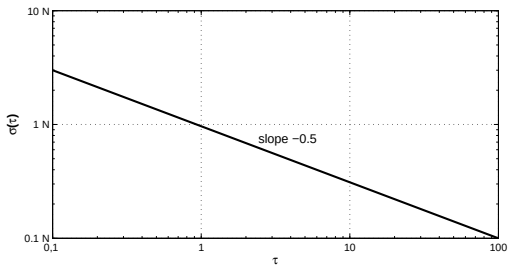

Figure 1: Angle random walk

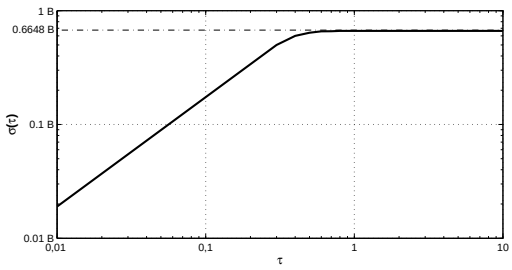

Figure 2: Bias instability

2.1.3 RATE RANDOM WALK (RRW)

Long term changes to bias offset will be randomly distributed and may be permanent in nature. Even though the drift of an individual sensor can not be predicted, the time scale over which the changes occur can be defined by the RRW and introduces the opportunity to plan for recalibration in critical applications that require extended life. The rate PSD associated with this noise is [1]:

$$S(f) = \frac{K^2}{2\pi f^2}, \tag{12}$$

where K means the RRW coefficient. By substituting (12) into (6) and performing the integration we get:

$$\sigma_{rrw}^2(\tau) = \frac{K^2}{3}\tau \tag{13}$$

This equation shows that RRW is represented by +0.5 slope on a log-log plot of $\sigma(\tau)$ (fig. 3). RRW constant K can be read off from plot at $\tau = 3$.

2.1.4 DRIFT RATE RAMP

This error belongs to deterministic errors. It is slow monotonic change of output over a long time period. It can be described as:

$$\omega(t) = Rt, \tag{14}$$

where R is the slope of ramp. AV characteristic is given by:

$$\sigma_{rr}^2(\tau) = \frac{R^2\tau^2}{2} \tag{15}$$

The slope in the log-log plot is +1 and the coefficient R can be read off at $\tau = \sqrt{2}$ (fig. 4).

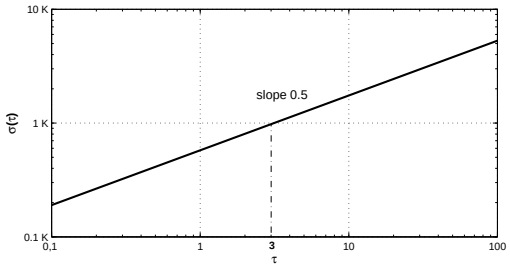

Figure 3: Rate random walk

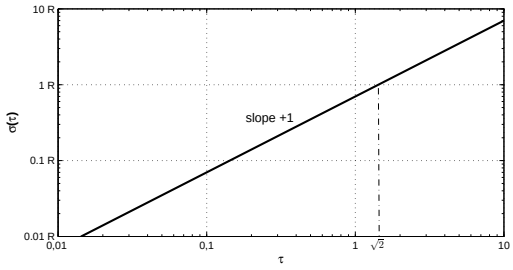

Figure 4: Drift rate ramp

3 MEASUREMENT DESCRIPTION

For a practical measurement, three different gyroscopes have been chosen: IvenSense IDG1215, Analog Devices ADXRS300EB and muRata ENV-05H. The measurement chain is compounded from a low-pass filter and data acquisition module (DAQ) NI-USB-6215. DAQ has a 16-bit analog to digital converter with a sampling frequency up to $250\,kS/s$. The sampling frequency was chosen $2\,kS/s$ with regard to the output frequency spectrum to satisfy the Nyquist theorem. The purpose of the low-pass filter is to suppress high frequency components in the spectrum. The cutoff frequency was chosen $600\,Hz$ (higher than a bandwidth of gyroscopes). Gyroscopes were powered from an accumulator with a linear regulator to eliminate problems with ground loops and a power supply interference. The purpose of the test is to describe a behavior without exciting the input, therefore gyroscopes were in a steady state without a motion during the measurement. The ambient temperature in a lab fluctuates between 22 and $25\,^{\circ}C$ in a period of 24 hours.

4 RESULTS

The figure 5 describes development of $\sigma(\tau)$ versus averaging time τ in a log-log scale. Data were collected for the interval of 72 hours to achieve a reliable estimate of the bias instability.

In the figure, we can see that ENV-05H has the best performance, because the bias instability is given by the lowest point on the AD curve. It is also obvious that level of ARW is much smaller in comparison to other two gyroscopes. On the other hand, the worst one in the test is the ADXRS300. The level of bias instability is more than ten times higher than the bias level of IDG1215. Also the output contains bigger amount of high frequency noise (ARW). When we focus on the performance of IDG1215 in each axis, we can see slight differences in levels of ARW and the bias instability. Estimated parameters for all gyroscopes are in the table 1.

In this comparison, the parameters of RRW and drift rate ramp were omitted. The reason is that output of gyroscopes is correlated with slow changes of the temperature in the lab. So the estimate of these parameters is unreliable.

Under the proper conditions the contribution of data acquisition module NI-USB-6215 to AV is more than ten times lower than measured values.

Gyroscope	N $[^\circ/\sqrt{s}]$	B $[^\circ/s]$
ENV-05H	$4.0 \cdot 10^{-4}$	$9.5 \cdot 10^{-4}$
IDG1215 (Y axis)	$3.0 \cdot 10^{-3}$	$13 \cdot 10^{-3}$
IDG1215 (X axis)	$3.2 \cdot 10^{-3}$	$14 \cdot 10^{-3}$
ADXRS300	$46 \cdot 10^{-3}$	$26 \cdot 10^{-3}$

Table 1: Estimated parameters

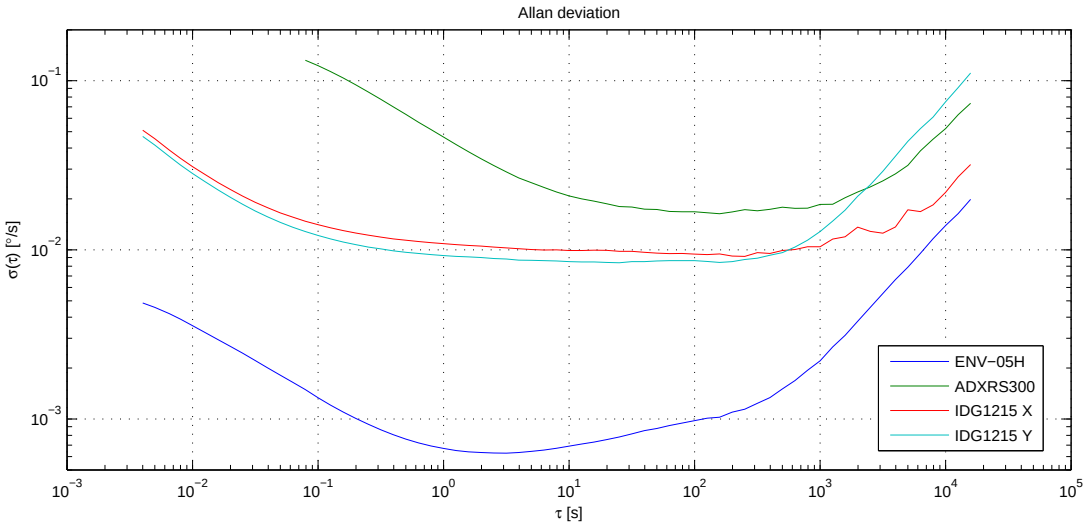

Figure 5: Allan deviation plot

5 CONCLUSION

This paper shows that the Allan variance is suitable to investigate the sensor error behaviors on different timescales and parameter estimation. Results show that for long-term measurements, the consideration of the ambient temperature influence is important. This problem should be solved by using a temperature chamber to keep the temperature steady during the measurement.

ACKNOWLEDGEMENT

This work was supported by grant “Modern Methods and Approaches in Automation” from the Internal Grant Agency of Brno University of Technology (grant No. FEKT-S-10-12).

REFERENCES

[1] IEEE standard specification format guide and test procedure for single-axis interferometric fiber optic gyros. IEEE Std 952-1997 (1998), i.

[2] Allan, D.: Statistics of atomic frequency standards. Proceedings of the IEEE 54, 2 (feb. 1966), 221–230.

[3] Ng, L. C.: On the application of Allan variance method for ring laser gyro performance characterization. Lawrence Livermore National Laboratory Report (1993).

[4] Tehrani, M.: Ring laser gyro data-analysis with cluster sampling technique. Proceedings of the SPIE the International Society for Optical Engineering 412 (1983), 207–220.